Concomitant wave and current effects on vortex-induced motion (VIM) of a large-volume semi-submersible platform

Conference Paper · June 2018

CITATIONS
0

READS
8

3 authors, including:

Rodolfo Trentin Gonçalves
The University of Tokyo
93 PUBLICATIONS **453** CITATIONS
SEE PROFILE

André L. C. Fujarra
Federal University of Santa Catarina, Joinville, Brazil
119 PUBLICATIONS **758** CITATIONS
SEE PROFILE

Proceedings of the Twenty-eighth (2018) International Ocean and Polar Engineering Conference
Sapporo, Japan, June 10-15, 2018

ISBN 978-1-880653-87-6; ISSN 1098-6189

www.isope.org

Concomitant wave and current effects on vortex-induced motion (VIM) of a large-volume semi-submersible platform

*Rodolfo Trentin Gonçalves**
Department of Naval Architecture and Ocean Engineering, Escola Politécnica, University of São Paulo
São Paulo, SP, Brazil

Leandro Assis Pinto
CENPES – Research and Development Center, Petrobras
Rio de Janeiro, RJ, Brazil

André Luís Condino Fujarra[+]
Department of Naval Architecture and Ocean Engineering, Escola Politécnica, University of São Paulo
São Paulo, SP, Brazil

*currently at the Department of Ocean Technology, Policy, and Environment, School of Frontier Sciences, The University of Tokyo
Kashiwa-shi, Chiba, Japan

[+]currently at the Department of Mobility Engineering, Federal University of Santa Catarina
Joinville, SC, Brazil

ABSTRACT

This research work aims to understand the behavior of large-volume semi-submersible platforms under the action of VIM and simultaneous wave incidence. VIM model tests with regular and irregular waves collinear to the current conditions were carried out to achieve the goals. The results showed that the waves influenced the phenomenon, although the nature of the wave (regular or irregular) was not the source of the VIM mitigation. The results were analyzed by using plots of velocity ratio α as function of the Keulegan–Carpenter number KC, which determines the force region predominance: inertia or viscous. The VIM was mitigated in results in the inertia-force region; yet it manifested even in low amplitudes for cases in the viscous-force region.

KEY WORDS: vortex-induced motions, wave incidence, semi-submersible, model tests.

NOMENCLATURE

A_y	nominal amplitude in the transverse direction
A_{yaw}	nominal amplitude of the yaw motion
C_a	added mass coefficient
C_D	drag coefficient
D	characteristic diameter
f_P	frequency of the peak
f_{RW}	frequency of the regular wave
H	column height above pontoon
H_{RW}	height of the regular wave
H_S	significant height
IW	irregular wave
KC	Keulegan–Carpenter number
KC_r	equivalent KC for irregular oscillatory flow
L	column face dimension
M	total mass
P	pontoon height
RW	regular wave
R_{XX}	radius of gyration in the X-axis
R_{YY}	radius of gyration in the Y-axis
R_{ZZ}	radius of gyration in the Z-axis
S	distance between column centers
T	draft
t	time
T_0	natural period of motion in the transverse direction in still water
T_P	wave period of peak
T_{RW}	period of the regular wave
U	incident current velocity
U_M	maximum flow velocity
U_w	oscillatory flow velocity
V_r	reduced velocity
X	direction along the X-axis
X_{CG}	position of the center of the gravity in the X-axis

Y	direction along the Y-axis
Y_{CG}	position of the center of the gravity in the Y-axis
Z	direction along the Z-axis
Z_{CG}	position of the center of the gravity in the Z-axis
α	velocity ratio
σ_U	RMS value of the fluid velocity of oscillatory flow

INTRODUCTION

VIM - vortex-induced motions is a particular way to call VIV - vortex-induced vibrations phenomenon. VIM occurs in offshore platforms due to current incidence. Motions in the transverse direction are in the same order of the platform main dimensions, see detailed review in Fujarra *et al.* (2012). These large amplitudes in the horizontal plane are responsible for decreasing the fatigue life of the mooring and riser systems. Therefore, VIM must be considered in the initial design phases, even for multi-column platforms, such as semi-submersible and TLP – tension-leg platforms. Some examples of experimental VIM studies on multi-columns can be found in Walls *et al.* (2007), Gonçalves *et al.* (2012, 2013, 2018) and Liu *et al.* (2016, 2017a, 2017b).

The study of the effects of the surface wave on VIM of offshore floating units is more recent. In practice, DNV rules (2007, 2008) discuss the impact of waves and current on VIM, and a conservative recommendation is to superimpose the forces calculated separately due to waves and vortex shedding. It is important to highlight that to quantify these phenomena together is not easy. This fact can increase the cost of the project and make the project unfeasible sometimes.

Another difficulty is the small number of references available about this subject in the open literature. Among the works discussing VIM together with wave incidence, van Dijk *et al.* (2003), Irani & Finn (2005) and Finnigan *et al.* (2005) on spar platforms; Cueva *et al.* (2006), Gonçalves *et al.* (2010) and Saito *et al.* (2012) on monocolumn platforms; and more recently, Rijken & Leverette (2008), Hong *et al.* (2008), Martin & Rijken (2012), Gonçalves *et al.* (2013), Pontaza *et al.* (2015), Koop *et al.* (2016) and Maximiano *et al.* (2017) on semi-submersibles can be cited.

Rijken & Leverette (2008) performed VIM tests on semi-submersible platforms with waves aligned to the current as a sea condition and concluded that the presence of waves time-delayed the onset of VIM; however, similar magnitude oscillations were observed. In the same way, Hong *et al.* (2008) carried out VIM tests with waves aligned to the current as a sea condition, and they concluded that the wave-induced particle velocity disturbs the VIM. Even so, few conditions were tested to answer the questions about wave effects. Moreover, Martin & Rijken (2012) investigated the impact of operational sea states on VIM; the authors showed that the operational sea state had minimal effect on the VIM response of a semi-submersible.

Gonçalves *et al.* (2013) performed VIM tests with three regular waves and three irregular waves (sea conditions) for the 45-deg incidence of a semi-submersible platform. Considerable differences between the presence of regular or irregular waves were observed. In the tests with regular waves, the motion amplitudes in the transverse direction were markedly lower than those with irregular waves, and the VIM behavior was not observed. In the sea state tests, the amplitudes were lower than current-only ones, yet a periodic motion characterized by VIM was verified. An in-depth study showed that the nature of the wave (regular or irregular) was not relevant to the VIM response; however, the oscillatory nature of the motions in the in-line direction was related to this influence. This effect could be quantified by the plots of α versus KC, where α is the velocity ratio and KC is the Keulegan–Carpenter number related to the motions in the in-line direction; details about this methodology are presented further on. The yaw amplitudes showed a small decrease in all the wave conditions performed.

Recently, Koop *et al.* (2016) and Maximiano *et al.* (2017) investigated the effect of different irregular wave conditions and different wave incidences, namely in-line, transverse and oblique waves concerning the current. The results suggested that the two most important factors that influence the VIM and waves were the wave height, and the relation between wave and current directions. A 15% reduction in the peak response was found for the smallest sea state when compared with the case without waves; however, with the highest significant wave height, the peak response was reduced by 30%. Depending on the combination of current-wave direction, the influence of the same sea state on VIM response can be negligible (transverse seas) or result in a 30% reduction of the peak response for collinear sea and current.

In this context, the purpose of the present research was to study the concomitant wave and current effects on the VIM of a large-volume semi-submersible platform. The methodology of analysis was the same proposed before by Gonçalves *et al.* (2013). VIM model tests were performed in the presence of 8 regular waves and also 8 different conditions of sea state, all of them aligned to the current.

Section 2 presents a summary of the methodology for analyzing the effects of surface waves. The experimental setup, details about the reduced scale model and wave conditions are described in Section 3. The results and comparison concerning characteristic motion amplitudes for motions in the transverse direction and yaw, as well as the plots ofα versus KC are discussed in Section 4. Finally, in Section 5, the conclusions are drawn.

METHODOLOGY

The methodology applied to understand the wave effects on the VIM of platforms was proposed in Gonçalves *et al.* (2013), and it will be detailed after some introduction of the essential parameters.

Another way to study the effect of the oscillating flow on vortex shedding is to impose oscillatory motions in the in-line direction of an elastically-mounted cylinder free to vibrate transversely, for example, the one studied by Sumer & FredsØe (1988), for regular oscillatory flow; and also by Kozakiewicz *et al.* (1994), for irregular condition. The transverse response depends on the ratio of frequencies of the oscillatory flow and the natural frequency of the system, f_{RW}/f_N; Keulegan-Carpenter number, KC; reduced velocity, V_r; and also on the Reynolds number.

As described in Sumer & FredsØe (1988), under regular (sinusoidal) oscillatory flow, the Keulegan-Carpenter number is defined by

$$KC = \frac{U_M}{f_{RW} D} \tag{1}$$

where $U_M$is the maximum flow velocity defined by:

$$U_w(t) = U_M sin(2\pi f_{RW} t) \tag{2}$$

On the other hand, as described in Kozakiewicz *et al.* (1994), under irregular oscillatory flow, the equivalent KC_r is defined by:

$$KC_r = \frac{\sqrt{2}\sigma_U}{f_P D} \tag{3}$$

where σ_U is the RMS value of the fluid velocity of oscillatory flow and f_P is the peak frequency of the flow.

A quasi wave-current co-existing field can be easily obtained either by oscillating a cylinder in the in-line direction in a uniform flow, as in Moreau & Huang (2010), or by moving it at a constant speed in a harmonically oscillating flow, as presented in Iwagaki & Asano (1984). Both methods showed that another important parameter besides KC is ratio α defined as:

$$\alpha = \frac{\sigma_U}{\sigma_U + U} \quad (4)$$

where U is the mean current velocity. This ratio becomes 1 at the limit of wave-only and tends to 0 as the current becomes large as compared with the oscillatory component. According to Iwagaki & Asano (1984), the plot of α as a function of the KC showed the ratio of viscous force to the inertia force. This result will be very important to understand the phenomenon of vortex-shedding and oscillatory flow, as discussed further on.

As detailed in Gonçalves *et al.* (2013) and summarized herein, the in-line motion due to the wave excitation can be considered the imposed oscillatory motion and its respective Keulegan-Carpenter number calculated using Eq. 1, for regular waves, and Eq. 3 for sea condition incidence. The effect of simultaneous current and waves is calculated using ratio α as in Eq. 4. The region of either drag or inertia force for the tests with simultaneous wave and current can be seen in the mentioned plot, as proposed in Iwagaki & Asano (1984). The limit curve represents the condition for the drag force (viscous) equal to the inertia force, which is calculated as:

$$KC = \frac{1 + C_a}{C_D}(\pi\alpha^2) \quad (5)$$

where C_a is the transverse (or in-line) added mass of the platform for a 45-degree incidence and C_D is the static drag coefficient for a 45-degree incidence. The values of these coefficients for the semi-submersible under study are $C_a \cong 0.76$ and $C_D \cong 0.75$, see Gonçalves *et al.* (2012).

The proposed methodology concluded that when the results fall within the inertia region, the wave excitation dominates over the vortex shedding; therefore, no VIM behavior is observed. Conversely, for the viscous drag region, the vortex-shedding phenomena dominate over the wave excitation; therefore, VIM is still present, albeit possibly reduced when compared to current alone conditions.

The current incidence angle tested was 45 degrees, the one presenting higher VIM amplitudes in the transverse direction. At least 6 different reduced velocities were tested for each condition of the coexistent wave. The reduced velocity is defined as

$$V_r = (U.T_0)/D \quad (6)$$

where U is the incident current velocity, T_0 is the natural period of motion in the transverse direction in still water and D is the characteristic length of the cross-section of the body subjected to a vortex shedding, i.e., $D = \sqrt{2}L$ for 45-degree incidence, where L is the face dimension of the column. The reduced velocity did not take the wave velocity into account, and the small difference due to the wave incidence can be neglected.

The VIM response was analyzed using the RMS - root mean square of displacements in the transverse direction and angles of rotation in the case of the yaw motion. The nominal amplitudes were calculated as $\sqrt{2}$ times the RMS amplitude. Moreover, as commonly found, dimensionless values A_y/L were presented using the face dimension of the column, L. For the RMS angles of yaw, A_{yaw}, no dimensionless presentation was adopted, as usual in the literature.

EXPERIMENTAL SETUP

The experimental setup is characterized by a small-scale model of the semi-submersible unit supported by a set of equivalent horizontal mooring lines in the towing tank at the IPT - Institute of Technological Research in São Paulo, Brazil.

The picture of the 1:100 scaled-model is presented in Fig. 1. The main characteristics of the platform model are shown in Table 1~2 and Fig. 2. The model was built with a ring located in the column portions above the water level to fix the equivalent mooring system, as can be seen in Fig 3. That ring allowed using the same mooring configuration for all different current incidences, i.e., the same value of mooring stiffness.

Fig 1. Picture of the model in the reduced scale.

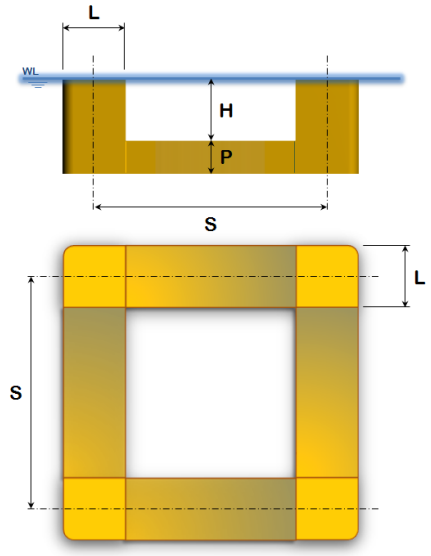

Fig 2. Illustration of the characteristic dimensions of the platform.

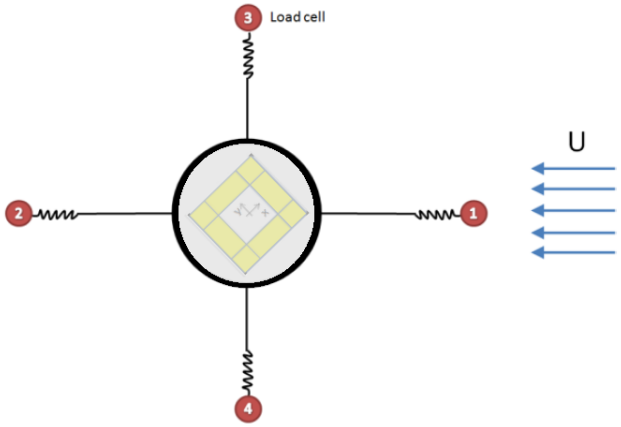

Fig 3. Sketch of the equivalent mooring system composed of four equivalent mooring lines for the 45-degree current incidence angle.

Table 1. Main characteristic dimensions values of the platform model. Dimensions are in the model scale.

SS-platform Characteristic	Value
Scale	1:100
Distance between columns (S)	745.2 mm
Column height above pontoon (H)	226.0 mm
Column length (L)	198.0 mm
Pontoon height (P)	114.0 mm
Draft ($T = P + H$)	335.3 mm

Table 2. Main inertia characteristic values of the platform model.

Parameter	Value
Total mass (M)	100.5 kg
X_{CG}	-0.3 mm
Y_{CG}	3.9 mm
Z_{CG}	246.1 mm
R_{XX}	385.7 mm
R_{YY}	361.2 mm
R_{ZZ}	426.1 mm

The current angle tested was 45-degree incidence, the one presenting the highest VIM amplitudes in the transverse direction without wave presence At least 6 different reduced velocities were tested for each condition of simultaneous presence of wave and current. Regular and irregular waves (sea conditions) were performed to verify the effects on VIM owing to the presence of energy in different frequency ranges.

Eight regular waves, described by period and height, were chosen to represent different responses in the RAO – response amplitude operator. Table 3 presents the characteristic parameters of the regular wave conditions performed.

The regular waves were selected to comprise the motions in the in-line direction in both regions, inertia and viscous forces, in the $\alpha - KC$ plot. The previous work by Gonçalves *et al.* (2013) comprised only regular waves in the inertia region, and all the results showed complete mitigation of the VIM phenomenon. The regular wave tests performed herein aimed to complement the previous work and confirm that the nature of the wave is not responsible for the VIM mitigation.

Table 3. Regular wave characteristics without current incidence. Values in the platform model scale 1:100.

ID	Condition	T_{RW} [s]	H_S [cm]
RW 1	Current + regular wave	1.1	4.0
RW 2	Current + regular wave	1.7	8.0
RW 3	Current + regular wave	3.0	10.0
RW 4	Current + regular wave	2.5	14.0
RW 5	Current + regular wave	3.0	4.0
RW 6	Current + regular wave	2.5	5.0
RW 7	Current + regular wave	3.0	3.0
RW 8	Current + regular wave	2.5	2.0

Table 4. JONSWAP irregular wave (sea conditions) characteristics without current incidence. Values in the platform model scale 1:100.

ID	Condition	T_P [s]	H_S [cm]
IW 1	Current + irregular wave	1.10	7.5
IW 2	Current + irregular wave	1.55	11.0
IW 3	Current + irregular wave	1.65	9.0
IW 4	Current + irregular wave	1.70	2.0
IW 5	Current + irregular wave	1.80	3.0
IW 6	Current + irregular wave	1.80	5.0
IW 7	Current + irregular wave	2.00	2.0
IW 8	Current + irregular wave	2.20	3.0

Similarly to the regular wave conditions, eight irregular waves described by a JONSWAP spectrum were chosen to represent different environmental conditions, corresponding to distinct levels of unit motion. Table 4 presents the characteristic parameters of the irregular wave conditions performed.

RESULTS

All the VIM response amplitudes with concomitant wave incidence were benchmarked with the case without wave incidence. By means of this approach one can directly visualize the wave effects on the VIM of the platform.

Figure 4 presents the nondimensional amplitudes for the motions in the transverse direction with and without regular wave presence. The results for cases RW1 to RW4 showed a decrease in amplitudes due to the regular wave incidence, mainly for the complete mitigation for cases RW1 to RW3. It is possible to highlight that this reduction occurred for the resonance range whereby the amplitudes had maximum values without wave incidence. However, the results for cases RW5 to RW8 were quite similar to those without waves; and in the particular cases RW5 and RW8, some amplitudes were higher than the respective ones without waves.

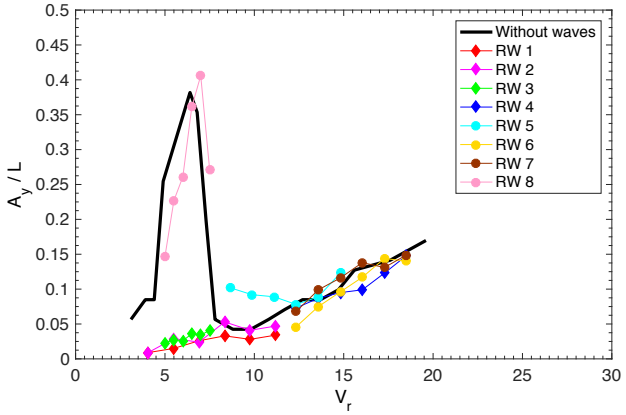

Fig 4. Nondimensional amplitudes for the motions in the transverse direction for the 45-degree current incidence: regular waves and without wave incidence.

Therefore, the results in Fig. 4 allowed concluding that the nature of the wave, regular ones in this case, is not responsible for mitigating the VIM phenomenon, since the regular wave conditions can reduce the amplitudes (RW1 to RW3) and also allow high amplitudes of VIM (RW5 and RW8).

These results were entirely new because, in Gonçalves *et al.* (2013), only regular wave conditions capable of mitigating the VIM phenomenon were performed.

The methodology of plot α versus KC was applied to the results in Fig. 4. The results $\alpha - KC$ plot are presented in Fig. 5, confirming that the cases of VIM mitigation (RW1 to RW4) were located in the predominant inertia region; this means that the inertia forces due to the regular wave incidence that promoted the motions in the in-line direction were more significant than the lift force due to the vortex-shedding around the platform; therefore, the VIM behavior is not present.

Conversely, the results in Fig. 5 also confirmed that the cases in which the VIM behavior is possible are located in the viscous region

(predominant drag forces). For the cases from RW5 to RW8, the viscous forces due to the vortex-shedding around the platform were large enough to promote the VIM amplitudes in the transverse direction, even higher amplitudes as compared with the case without waves.
By analyzing Fig. 4 and Fig. 5 together, the methodology proposed in Gonçalves *et al.* (2013) and the use of plot α versus KC for determining the possibility of the occurrence of the VIM phenomenon was useful and can be applied to the preliminary investigations of the concomitant VIM phenomenon and wave incidence.

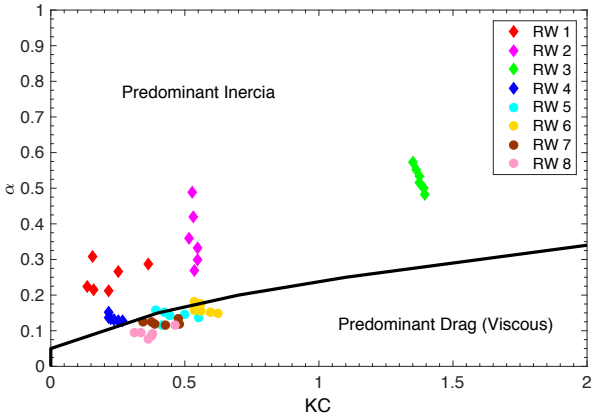

Fig 5. $\alpha - KC$ plot: predominant region of either drag or inertia force using the in-line motion as the imposed oscillatory motion due to the regular wave incidence.

Figure 6 presents the yaw characteristic amplitudes with and without regular wave presence. As verified previously in Gonçalves *et al.* (2013), the regular waves did not influence this degree of freedom significantly. In general, these results corroborated the notion that the wave incidence slightly decreases the yaw amplitudes.

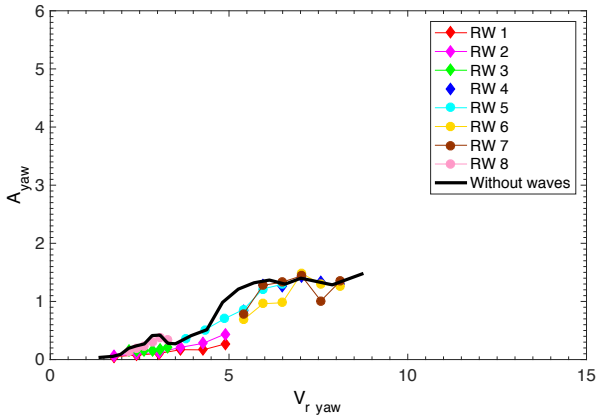

Fig 6. Yaw characteristic amplitudes for the 45-degree current incidence: regular waves and without wave incidence.

Figure 7 presents the nondimensional amplitudes for the motions in the transverse direction with and without irregular wave (sea condition) presence. The results for cases IW1 to IW3 showed a decrease of the amplitudes in the transverse direction, but not the complete mitigation of the VIM response. However, the results for cases IW4 to IW8a showed similar amplitude values and a shift to the right in the reduced velocity due to the increase in the horizontal plane velocity owing to the wave contribution. The results for case IW8b are for high values of reduced velocity in which the VIM synchronization is not observed; a dominant motion frequency cannot be defined, either.
Therefore, the results in Fig. 7 also allowed concluding that the nature of the irregular waves is not responsible for mitigating the VIM phenomenon, since the irregular wave conditions could substantially decrease the amplitudes (IW1 to IW3) and also allow similar high amplitudes of VIM (IW4 and IW8) as compared with the case without waves.

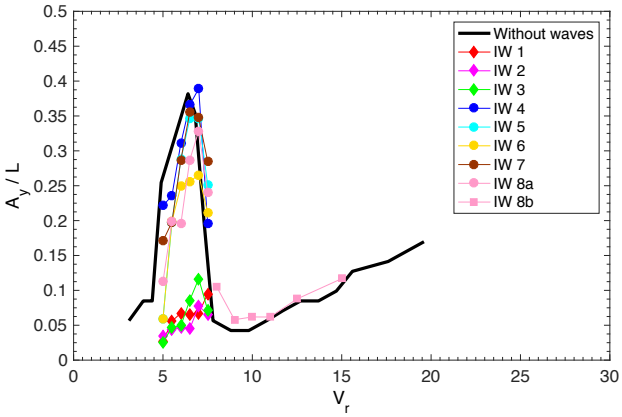

Fig 7. Nondimensional amplitudes for the motions in the transverse direction for the 45-degree current incidence: irregular waves (sea conditions) and without wave incidence.

Again, the methodology of plot α versus KC was applied to the results in Fig. 7. The results $\alpha - KC$ plot are presented in Fig. 8. All the results for the irregular waves were located in the predominant viscous (drag) forces, except for IW8 situated on the threshold of the regions. The results for IW1 to IW3 were expected to be located at the predominant inertia forces due to the substantial decrease in the amplitudes of the motions in the transverse direction, but these results were not confirmed.

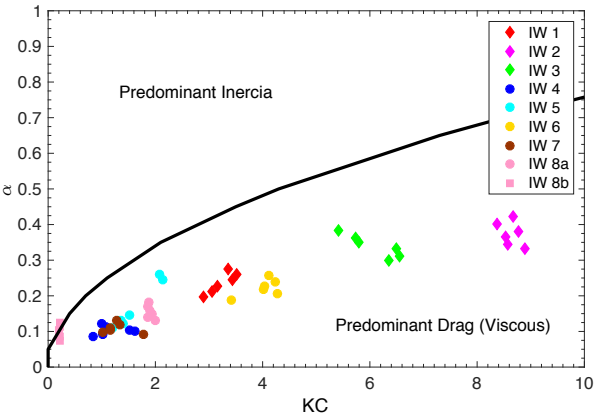

Fig 8. $\alpha - KC$ plot: predominant region of either drag or inertia force using the in-line motion as the imposed oscillatory motion due to the irregular waves (sea conditions) incidence.

The VIM phenomenon is characterized by motion amplitudes around the frequencies of the platform natural frequencies in the horizontal plane. The results for IW1 to IW3 still present the dominant frequency around the platform natural frequencies in the natural plane, which characterized the VIM phenomenon even for low amplitudes in the transverse direction. In cases RW1 to RW4, it was not possible to verify energy around the natural frequencies; thus, no VIM phenomenon existed. Only energy in the regular wave frequency was observed. Hence, the $\alpha - KC$

plot is capable of inferring the existence or not of the VIM phenomenon, but the plot does not allow explaining how large the effect of the waves is and how the amplitude of the VIM phenomenon can be modified in case VIM exists (points in the predominant viscous forces).

By analyzing Fig. 7 and Fig. 8 together, the proposition made by Gonçalves *et al.* (2013) and the use of plot α versus KC for determining the possibility of the VIM phenomenon to occur for regular and irregular wave conditions showed to be an appropriate procedure.

Fig. 9 presents the yaw characteristic amplitudes with and without irregular wave presence. As verified previously, irregular waves did not influence this degree of freedom significantly.

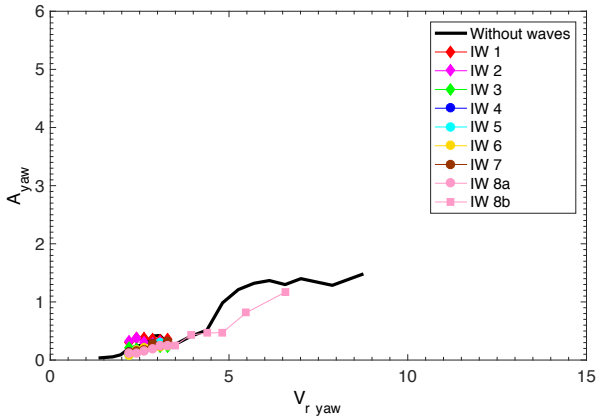

Fig 9. Yaw characteristic amplitudes for the 45-degree current incidence: irregular waves (sea conditions) and without wave incidence.

Some points need to be further investigated. For example, it is necessary to understand the level of mitigation of the VIM phenomenon for the cases in the predominant viscous (drag) forces, since the irregular waves did not show the complete mitigation of the VIM. The motions in other degrees of freedom (heave, roll, and pitch) are expected to also perturb the flow and wake around the platform and to promote different viscous forces, as pointed out before by other authors, for example Finnigan *et al.* (2005) and Gonçalves *et al.* (2010).

CONCLUSIONS

VIM model tests in waves were carried out. Regular and irregular wave conditions were performed to understand the effect of these environments on the VIM phenomenon.

The methodology previously proposed in Gonçalves *et al.* (2013) was now extensively applied to verify the VIM existence due to the wave presence. The method suggested using the $\alpha - KC$ plot considering the motions in the in-line direction caused by the wave incidence. The aims of the $\alpha - KC$ plot were to locate the results in the predominant inertia or predominant viscous (drag force). According to the graph, it is possible to evaluate the VIM existence in the case of results located in the predominant viscous region, or the non-existence of the VIM in the case of results located in the predominant inertia region.

The results of amplitudes in the transverse direction and $\alpha - KC$ plot for regular and irregular wave proved that the procedure is valid, but not enough to know the level of the VIM mitigation. The motions in the other degrees of freedom outside the horizontal plane should be taken into account in further works.

Also, the results corroborate that the wave nature, regular or irregular, was not the responsible for the VIM mitigation.

This procedure can be useful to update the current DNV rules, and also help designers in the early stages, since the wave effects on the VIM phenomenon could be better analyzed.

ACKNOWLEDGEMENTS

The first author would like to thank the São Paulo Research Foundation (FAPESP), process number 2014/02043-1, for supporting an important part of the VIM researches at USP. The Brazilian National Council for Research (CNPq) is acknowledged by the second author for grant 304600/2016-4. The authors also thank engineers Figueiredo, FP, Gambarine, DM, Amorim, FV, Momenti, AM, and Chame, MEF for their help in performing the tests.

REFERENCES

Cueva, M, Fujarra, ALC, Nishimoto, K, Quadrante, L, and Costa, A (2006) "Vortex induced motion: model testing of a monocolumn floater," *Proc of the ASME 2006 25th International Conference on Offshore Mechanics and Arctic Engineering*, OMAE2006-92167, Hamburg, Germany.

DNV (2007) "Recommended Practice DNV-RP-C205 – Environmental Conditions and Environmental Loads".

DNV (2008). "Offshore Standard DNV-OS-E301 – Position Mooring".

Dijk, RR, Magee, A, Perryman, S, and Gebara, J (2003). "Model test experience on vortex induced vibrations of truss spars," *Proc of the Offshore Technology Conference (OTC 2003)*, OTC2003-15242, Houston, USA.

Finnigan, T, Irani, M, and Dijk, R (2005) "Truss spar VIM in waves and currents," *Proc of the ASME 2005 24th International Conference on Offshore Mechanics and Arctic Engineering,* OMAE2005-67054, Halkidiki, Greece.

Fujarra, ALC, Rosetti, GF, Wilde, J, and Gonçalves, RT (2012) "State-of-art on vortex-induced motion: A comprehensive survey after more than one decade of experimental investigation," *Proc of the ASME 2012 31st International Conference on Ocean, Offshore and Arctic Engineering*, OMAE2012-83561, Rio de Janeiro, RJ, Brazil.

Gonçalves, RT, Fujarra, ALC, Rosetti, GF, and Nishimoto, K (2010). "Mitigation of vortex-induced motion (VIM) on a monocolumn platform: forces and movements," *Journal of Offshore Mechanics and Arctic Engineering*, 132(4), pp. 041102.

Gonçalves, RT, Rosetti, GF, Fujarra, ALC, and Oliveira, AC (2012) "Experimental study on vortex-induced motions of a semi-submersible platform with four columns, Part I: Effects of current incidence angle and hull appendages," *Ocean Engineering*, 54, pp. 150-169.

Gonçalves, RT, Rosetti, GF, Fujarra, ALC, and Oliveira, AC (2013) "Experimental study on vortex-induced motions of a semi-submersible platform with four columns, Part II: Effects of surface waves, external damping and draft condition," *Ocean Engineering*, 62, pp. 10-24.

Gonçalves, RT, Fujarra, ALC, Rosetti, GF, Kogishi, AM, and Koop, A (2018) "Experimental study of the column shape and the roughness effects on the vortex-induced motions of deep-draft semi-submersible platforms," *Ocean Engineering*, 149, pp. 127-141.

Hong, Y, Choi, Y, Lee, J, and Kim, Y (2008) "Vortex-induced motion of a deep-draft semi-submersible in current and waves," *Proc of the 18th International Offshore and Polar Engineering Conference (ISOPE2008)*, Vancouver, BC, Canada.

Irani, M, and Finn, L (2005) "Improved strake design for vortex induced motions of spar platforms," *Proc of the ASME 2005 24th International Conference on Offshore Mechanics and Arctic Engineering*, OMAE2005-67384, Halkidiki, Greece.

Iwagaki, Y, and Asano, T (1984) "Hydrodynamic forces on a circular cylinder due to combined wave and current loading", *Proc of the International Conference on Coastal Engineering*, 19.

Koop, A, Wilde, J, Fujarra, ALC, Rijken, O, Linder, S, Lennblad, J, Haug, N, and Phadke, A (2016) "Investigation on reasons for possible

difference between VIM response in field and in model tests," *Proc of the ASME 2016 35th International Conference on Ocean, Offshore and Arctic Engineering*, OMAE2016-54746, Busan, South Korea.

Kozakiewicz, A, Sumer, BM, and FredsØe, J (1994) "Cross-flow vibrations of cylinder in irregular oscillatory flow," *Journal of Waterway, Port, Coastal, and Ocean Engineering*, 120, pp. 515-534.

Liu, M, Xiao, L, Lu, H, and Shi, J (2016) "Experimental investigation into the influences of pontoon and column configuration on vortex-induced motions of deep-draft semi-submersibles," *Ocean Engineering*, 123, pp. 262-277.

Liu, M, Xiao, L, Liang, Y, and Tao, L (2017a) "Experimental and numerical studies of the pontoon effect on vortex-induced motions of deep-draft semi-submersibles," *Journal of Fluids and Structures*, 72, pp. 59-79.

Liu, M, Xiao, L, Lu, H, and Xiao, X (2017b) "Experimental study on vortex-induced motions of a semi-submersible with square columns and pontoons at different draft conditions and current incidences," *International Journal of Naval Architecture and Ocean Engineering*, 9, pp. 326-338.

Martin, B, and Rijken, O (2012) "Experimental analysis of surface geometry, external damping and waves on semisubmersible vortex induced motions," *Proc of the ASME 2012 31st International Conference on Ocean, Offshore and Arctic Engineering*, OMAE2012-83689, Rio de Janeiro, Brazil.

Maximiano, A, Koop, A, Wilde, J, and Gonçalves, RT (2017) "Experimental study on the vortex-induced motions (VIM) of a semi-submersible floater in waves," *Proc of the ASME 2017 36th International Conference on Ocean, Offshore and Arctic Engineering*, OMAE2017-61543, Trondheim, Norway.

Pontaza, J, Baar, J, and Liu, N (2015) "Vortex-induced motions of a model scale column stabilized floater with round columns in calm water and random waves," *Proc of the ASME 2015 34th International Conference on Ocean, Offshore and Arctic Engineering*, OMAE2015-42407, St. John's, NL, Canada.

Rijken, O, and Leverette, S (2008) "Experimental study into vortex induced motion response of semi submersible with square columns," *Proc of the ASME 2008 27th International Conference on Offshore Mechanics and Arctic Engineering*, OMAE2008-57396, Estoril, Portugal.

Saito, M, Masanobu, S, Taniguchi, T, Otsubo, K, Asanuma, T, and Maeda, K (2012) "Experimental evaluation of VIM on MPSO in combined environmental conditions for waves and current," *Proc of the ASME 2012 31st International Conference on Ocean, Offshore and Arctic Engineering*, OMAE2012-83283, Rio de Janeiro, RJ, Brazil.

Sumer, BM, and FredsØe, J (1988) "Transverse vibration of an elastically mounted cylinder exposed to an oscillating flow," *Journal of Offshore Mechanics and Arctic Engineering*, 110, pp. 387-394.

Waals, OJ, Phadke, AC, and Bultema, S (2007) "Flow Induced Motions of Multi Column Floaters," *Proc of the ASME 2007 26th International Conference on Offshore Mechanics and Arctic Engineering*, OMAE2007-29539, San Diego, California, USA.